Vol 13 No 12, December 2004
1009-1963/2004/13(12)/2030-08

Chinese Physics

© 2004 Chin. Phys. Soc.
and IOP Publishing Ltd

Ground state properties of a Bose–Einstein condensate confined in an anharmonic external potential*

Wang Deng-Long(王登龙)[a], Yan Xiao-Hong(颜晓红)[a)b)†], and Tang Yi(唐 翌)[a]

[a] *Department of Physics and Key Laboratory for Advanced Materials and Rhelogical Properties of Ministry of Education, Xiangtan University, Xiangtan* 411105, *China*

[b] *College of Science, Nanjing University of Aeronautics and Astronautics, Nanjing* 210016, *Jiangsu, China*

(Received 9 May 2003; revised manuscript received 30 July 2004)

In light of the interference experiment of Bose–Einstein condensates, we present an anharmonic external potential model to study ground state properties of Bose–Einstein condensates. The ground state energy and the chemical potential have been analytically obtained, which are lower than those in harmonic trap. Additionally, it is found that the anharmonic strength of the external potential has an important effect on density and velocity distributions of the ground state for the Thomas–Fermi model.

Keywords: Bose–Einstein condensates, anharmonic external potential, ground state properties
PACC: 0530J, 3280, 6460

1. Introduction

The realization of experimental observations for ^{87}Rb,[1] ^{23}Na,[2] and ^{7}Li[3–6] condensates, which reveals various interesting phenomena, has renewed theoretical and experimental interest in quantum many-body systems at extremely low temperatures.[7,8] In these experiments, the vapours of alkali atoms are very dilute. One recognizes that the s-wave scattering length of the condensate is much less than the average distance among atoms.[9] As a consequence, one often uses Gross–Pitaevskii theory[10–12] to analyse the characteristics of Bose–Einstein condensate (BEC), where the basic equation, namely the Gross–Pitaevskii equation (GPE) describing the condensate wavefunction $\Psi(\boldsymbol{r},t)$, is generally given by[9,13]

$$\mathrm{i}\hbar\frac{\partial\Psi(\boldsymbol{r},t)}{\partial t}=\Big[-\frac{\hbar^2}{2m}\nabla^2+V_{\mathrm{trap}}(\boldsymbol{r})+U_0|\Psi(\boldsymbol{r},t)|^2\Big]\Psi(\boldsymbol{r},t),\qquad(1)$$

with external potential $V_{\mathrm{trap}}(\boldsymbol{r})$ and interatomic interaction strength $U_0 = 4\pi\hbar^2 Na/m$ (a is scattering length). By defining a harmonic external potential[14,15]

$$V_{\mathrm{trap}}(\boldsymbol{r})=\frac{1}{2}m(\omega_\perp^2x^2+\omega_\perp^2y^2+\omega_z^2z^2),\qquad(2)$$

where $\omega_\perp$ and ω_z are respectively the components of angular frequency $\boldsymbol{\omega}$ in the x–y plane and z direction, the bosons confined in isotropic[16,17] and anisotropic traps[18–23] can be described. For instance, by simple scaling arguments, Baym and Pethick[14] showed that the kinetic energy can be regarded as a small perturbation when the number of particles becomes large enough, and found that a spatial structure of atomic clouds and the momentum distribution are closely dependent on atomic interactions.

Recently, Andrews *et al*[24] observed interference patterns associated with phase coherence, while Anderson *et al*[25] showed the interference of atomic de Broglie waves tunnelling from a vertical array of macroscopically populated traps. In these experiments, the traps were located at the antinodes of an optical standing wave and loaded from a BEC. Subsequently, several works[26,27] regarded this kind of trap

*Project supported by the Key Foundation for Science & Technology from the Ministry of Education of China (Grant No 204099) and partly by the Scientific Research Foundation of the Education Bureau of Hunan Province, China (Grant Nos 03C466 and 03A06).

†E-mail: xhyan@xtu.edu.cn

as a type of independent harmonic trap. Even though this presumption is certainly different from the case of real traps, it provides a simple and convenient way to study the ground state of BEC with repulsive interparticle interaction. Here, we present an anharmonic external potential

$$V_{\rm trap}(\boldsymbol{r}) = \frac{1}{2}m(\omega_\perp^2 x^2 + \omega_\perp^2 y^2 + \omega_z^2 z^2) - \frac{1}{2}\varepsilon[m(\omega_\perp^2 x^2 + \omega_\perp^2 y^2 + \omega_z^2 z^2)]^2 \quad (3)$$

to describe the properties of bosons in this kind of trap, where ε is a small positive parameter. For $\varepsilon > 0$, obviously, the corresponding potential curve of Eq.(3) represents a double-well (anharmonic) trap, which is similar to that of the experimental external potentials described in Ref.[25]; if $\varepsilon \leq 0$, its profile is a single-well (harmonic) trap.

This paper is organized as follows. In Section 2, we derive the Euler–Lagrange equation of the BEC confined in an anharmonic potential. Subsequently, by applying perturbation theory, we obtain the eigenstate and the aspect ratio of average velocity distribution under the condition without interatomic interaction in Section 3. In Section 4, by means of the Thomas–Fermi model, we have the analytic solution of the ground state wavefunction in strong interparticle interaction. Some interesting calculations and discussions are shown in Section 5. Section 6 is a brief summary.

2. Derivation of the dynamic equation

As is known, the total number of atoms in the condensate is a pseudo-constant related to the low thermal equilibrium temperature,[28] although the atoms in different wells can jump over a finite-height barrier between two wells into each other.[29,30] This means that the bosons would have a unified chemical potential μ at low temperatures.[31] So the mean-field theory is still valid. Decomposing the condensate wavefunction as $\Psi(\boldsymbol{r},t) = \Psi(\boldsymbol{r})\exp(-\mathrm{i}\mu t/\hbar)$, the GPE of the BEC confined in an anharmonic external potential is

$$\Big\{ -\frac{\hbar^2}{2m}\nabla^2 + \frac{1}{2}m(\omega_\perp^2 x^2 + \omega_\perp^2 y^2 + \omega_z^2 z^2) - \frac{1}{2}\varepsilon m^2(\omega_\perp^2 x^2 + \omega_\perp^2 y^2 + \omega_z^2 z^2)^2 + U_0|\Psi(\boldsymbol{r})|^2 \Big\}\Psi(\boldsymbol{r}) = \mu\,\Psi(\boldsymbol{r}). \quad (4)$$

For simplicity, we define the standard lengths as[13,15]

$$l_\perp = \left(\frac{\hbar}{m\omega_\perp}\right)^{1/2}, \quad l_z = \left(\frac{\hbar}{m\omega_z}\right)^{1/2}. \quad (5)$$

Then, the state factors of spatial coordinate, chemical potential and wavefunction are rescaled respectively as

$$\boldsymbol{r} = l_\perp \boldsymbol{r}_1, \mu = \mu_1\hbar\omega_\perp, \Psi(\boldsymbol{r}) = \sqrt{\frac{N}{l_\perp^3}}\,\Psi_1(\boldsymbol{r}_1). \quad (6)$$

Substituting Eqs.(5) and (6) into Eq.(4), the Euler-Lagrange equation can be written as

$$-\nabla_1^2\Psi_1(\boldsymbol{r}_1) + [(r_{\perp 1}^2 + \lambda^2 z_1^2) - \varepsilon_1(r_{\perp 1}^4 + 2\lambda^2 r_{\perp 1}^2 z_1^2 + \lambda^4 z_1^4)]\Psi_1(\boldsymbol{r}_1) + U_1|\Psi_1(\boldsymbol{r}_1)|^2\Psi_1(\boldsymbol{r}_1) = 2\mu_1\Psi_1(\boldsymbol{r}_1), \quad (7)$$

where $\lambda = \omega_z/\omega_\perp$, $U_1 = (2m/l_\perp\hbar^2)U_0$ and $\varepsilon_1 = \varepsilon\hbar\omega$.

3. Noninteracting model

As is well known, when the number of atoms in the condensate is small enough to neglect the interatomic interaction, Eq.(7) is turned into a stationary linear Schrödinger equation

$$-\nabla_1^2\Psi_1(\boldsymbol{r}_1) + [(r_{\perp 1}^2 + \lambda^2 z_1^2) - \varepsilon_1(r_{\perp 1}^4 + 2\lambda^2 r_{\perp 1}^2 z_1^2 + \lambda^4 z_1^4)]\Psi_1(\boldsymbol{r}_1) = 2\mu_1\Psi_1(\boldsymbol{r}_1). \quad (8)$$

Considering that ε_1 in Eq.(3) is a small constant, we can solve Eq.(8) by perturbation theory. Since $\hat{H}^{(1)} = \varepsilon_1(r_{\perp 1}^4 + 2\lambda^2 r_{\perp 1}^2 z_1^2 + \lambda^4 z_1^4)$ is regarded as a perturbation term, we have

$$-\nabla_1^2\Psi_1^{(0)}(\boldsymbol{r}_1) + (r_{\perp 1}^2 + \lambda^2 z_1^2)\Psi_1^{(0)}(\boldsymbol{r}_1) = E_1^{(0)}\Psi_1^{(0)}(\boldsymbol{r}_1). \quad (9)$$

The eigenenergy of the linear Schrödinger equation (9) is easily calculated

$$E_1 = n_x + n_y + 1 + \lambda\left(n_z + \frac{1}{2}\right), \quad (10)$$

where $E_1 = E/\hbar\omega_\perp$. Correspondingly, the eigenwavefunction is given by

$$\Psi_1 = CH_{n_x}H_{n_y}H_{n_z}\exp\left[-\frac{1}{2}(r_{\perp 1}^2 + \lambda z_1^2)\right], \quad (11)$$

where C and $H_{n_i}(i = x, y, z)$ represent the normalized constant and Hermitian polynomial, respectively. For the ground state, $n_x = n_y = n_z = 0$, we obtain $E_1^{(0)} =$

$1+\frac{\lambda}{2}$, and $\Psi_1^{(0)}=\lambda^{1/4}\pi^{-3/4}\exp\Big[-\frac{1}{2}(r_{\perp 1}^2+\lambda z_1^2)\Big]$. Consequently, one may obtain

$$E_1^{(1)}=\int(\Psi_1^{(0)})^*\hat{H}^{(1)}\Psi_1^{(0)}\mathrm{d}\boldsymbol{r}_1 =-\left(2+\lambda+\frac{3}{4}\lambda^2\right)\varepsilon_1. \quad (12)$$

From Eq.(10), some lower energies obtained are

$$E_n^{(1)}=\left(2+\frac{\lambda}{2}\right),\quad E_n^{(2)}=\left(1+\frac{3\lambda}{2}\right),$$

$$E_n^{(3)}=\left(3+\frac{\lambda}{2}\right),\quad E_n^{(4)}=\left(2+\frac{3\lambda}{2}\right),$$

$$E_n^{(5)}=\left(3+\frac{3\lambda}{2}\right),\quad E_n^{(6)}=\left(1+\frac{5\lambda}{2}\right)\cdots$$

By adding the normalization condition to Eq.(11), some corresponding lower wavefunctions are

$$\Psi_n^{(1)}=2^{1/2}\lambda^{1/4}\pi^{-3/4}r_{\perp 1}\cos\theta\exp\Big[-\frac{1}{2}(r_{\perp 1}^2+\lambda z_1^2)\Big]$$

or

$$2^{1/2}\lambda^{1/4}\pi^{-3/4}r_{\perp 1}\sin\theta\exp\Big[-\frac{1}{2}(r_{\perp 1}^2+\lambda z_1^2)\Big],$$

$$\Psi_n^{(2)}=2^{1/2}\lambda^{1/4}\pi^{-3/4}z\exp\Big[-\frac{1}{2}(r_{\perp 1}^2+\lambda z_1^2)\Big],$$

$$\Psi_n^{(3)}=\lambda^{1/4}\pi^{-3/4}r_{\perp 1}^2\sin\theta\exp\Big[-\frac{1}{2}(r_{\perp 1}^2+\lambda z_1^2)\Big],$$

$$\Psi_n^{(4)}=2\lambda^{3/4}\pi^{-3/4}zr_{\perp 1}\cos\theta\exp\Big[-\frac{1}{2}(r_{\perp 1}^2+\lambda z_1^2)\Big]$$

or

$$2\lambda^{3/4}\pi^{-3/4}zr_{\perp 1}\sin\theta\exp\Big[-\frac{1}{2}(r_{\perp 1}^2+\lambda z_1^2)\Big],$$

$$\Psi_n^{(5)}=2^{1/2}\lambda^{3/4}\pi^{-3/4}zr_{\perp 1}^2\sin 2\theta\exp\Big[-\frac{1}{2}(r_{\perp 1}^2+\lambda z_1^2)\Big],$$

$$\Psi_n^{(6)}=\frac{1}{\sqrt{2}}\lambda^{3/4}\pi^{-3/4}(4z^2-2)\left(\frac{1}{\sqrt{1-\lambda}}\right)\times\exp\Big[-\frac{1}{2}(r_{\perp 1}^2+\lambda z_1^2)\Big]\cdots$$

The first correction of ground state wavefunction is

$$\Psi_1^{(1)}=\sum_{m=2}^{\infty}\frac{H'_{m1}}{E_1^{(0)}-E_m^{(0)}}\Psi_1^{(0)} =-\sqrt{2}\varepsilon_1(2+\lambda)\lambda^{1/4}\pi^{-3/4}\times\exp\Big[-\frac{1}{2}(r_{\perp 1}^2+\lambda z_1^2)\Big]. \quad (13)$$

As a result, the energy and wavefunction of the ground state are respectively given by

$$E_1=1+\frac{\lambda}{2}-(2+\lambda+\frac{3}{4}\lambda^2)\varepsilon_1, \quad (14)$$

$$\Psi_1=\lambda^{1/4}\pi^{-3/4}\exp\Big[-\frac{1}{2}(r_{\perp 1}^2+\lambda z_1^2)\Big]\times[1-\sqrt{2}\varepsilon_1(2+\lambda)]. \quad (15)$$

Furthermore, the average values $\langle x_1^2\rangle$ and $\langle z_1^2\rangle$ are

$$\langle x_1^2\rangle=\frac{1}{2}[1-2\sqrt{2}(2+\lambda)\varepsilon_1], \quad (16)$$

$$\langle z_1^2\rangle=\frac{1}{2\lambda}[1-2\sqrt{2}(2+\lambda)\varepsilon_1]. \quad (17)$$

The aspect ratio R is then derived by

$$R\equiv\sqrt{\frac{\langle p_z^2\rangle}{\langle p_x^2\rangle}}=\sqrt{\frac{\langle x_1^2\rangle}{\langle z_1^2\rangle}}=\sqrt{\lambda}, \quad (18)$$

which characterizes the anisotropy of the velocity distribution.[15]

4. Strong interaction limit

In the case that interatomic interaction increases as the number of atoms increases, Eq.(7) is hardly able to reduce to the linear Schrödinger equation (8). When the interatomic interaction energy is large enough, the kinetic energy can be neglected, and Eq.(7) is simplified:

$$|\Psi_1(\boldsymbol{r}_1)|^2=\frac{1}{U_1}[2\mu_1-(r_{\perp 1}^2+\lambda^2 z_1^2)+\varepsilon_1(r_{\perp 1}^4+2\lambda^2 r_{\perp 1}^2 z_1^2+\lambda^4 z_1^4)], \quad (19)$$

which is just the Thomas–Fermi model. Obviously, the right-hand side of Eq.(19) can be positive or zero, that is

$$2\mu_1-(r_{\perp 1}^2+\lambda^2 z_1^2)+\varepsilon_1(r_{\perp 1}^4+2\lambda^2 r_{\perp 1}^2 z_1^2+\lambda^4 z_1^4)\geq 0. \quad (20)$$

Applying the variance approach[32,33] to Eq.(20), we have

$$|z_1|\leq b=\frac{1}{\lambda}(2\mu_1+r_{\perp 1}^2)^{1/2}\left[1-\frac{1}{2}\varepsilon_1 r_{\perp 1}^2-\varepsilon_1\mu_1+\frac{\varepsilon_1 r_{\perp 1}^4}{2(2\mu_1-r_{\perp 1}^2)}\right]. \quad (21)$$

By normalizing the wavefunction,[14,15] i.e. $\int |\Psi_1|^2 \mathrm{d}\boldsymbol{r}_1 = 1$, the chemical potential μ_1 can be obtained from Eq.(19) as

$$\mu_1 \approx \frac{1}{2}\left(\frac{15\lambda U_1}{8\pi}\right)^{2/5}\left[1-\frac{3}{7}\varepsilon_1\left(\frac{15\lambda U_1}{8\pi}\right)^{2/5}\right], \quad (22)$$

with the corresponding coordinates $|r_1| \leq \sqrt{2\mu_1}$, $0 \leq \theta \leq 2\pi$, and $|z_1| \leq b$. With $\mu_1 = \mathrm{d}E_1/\mathrm{d}N$,[15] the average total energy is given by

$$E_1 = \int \mu_1 \mathrm{d}N \approx \frac{5}{14}\left(\frac{15\lambda a}{l_\perp}\right)^{2/5} N^{7/5} \times \left[1-\frac{1}{3}\varepsilon_1\left(\frac{15\lambda a N}{l_\perp}\right)^{2/5}\right]. \quad (23)$$

According to Eqs.(16) and (17), one obtains average values $\langle x_1^2\rangle$ and $\langle z_1^2\rangle$

$$\langle x_1^2\rangle = \frac{2}{7}\mu_1\left[1+\frac{110}{63}\varepsilon_1\mu_1\right], \quad (24)$$

$$\langle z_1^2\rangle = \frac{2}{7}\frac{\mu_1}{\lambda^2}\left[1+\frac{13}{7}\varepsilon_1\mu_1\right], \quad (25)$$

and then the aspect ratio

$$R \equiv \sqrt{\frac{\langle p_z^2\rangle}{\langle p_x^2\rangle}} = \sqrt{\frac{\langle x_1^2\rangle}{\langle z_1^2\rangle}} \approx \lambda\left(1-\frac{1}{18}\varepsilon_1\mu_1\right). \quad (26)$$

Obviously, the aspect ratio of BEC in an anharmonic external potential is related to ε_1, μ_1 and λ. This means that the strength of the anharmonic external potential has an important effect on the aspect ratio of BEC.

5. Results and discussions

As typical examples, we calculate the spatial distributions of density and the aspect ratio of velocity distributions of atoms of ^{87}Rb, ^{7}Li and H. ^{87}Rb and ^{7}Li are examples of the atoms with repulsive and attractive interactions, respectively. Owing to the simplicity of the hydrogen atom, properties such as interatomic potentials and spin relaxation rates have been well understood theoretically, hydrogen condensates share many characteristics with condensates of alkali metal atoms, but there are several notable differences because of hydrogen's small mass. The parameters of condensates ^{87}Rb, ^{7}Li and H are listed in Table 1, taken from the experiments in Refs.[1,3,34].

Table 1. Correlative parameters of ^{87}Rb, ^{7}Li and H atoms where a_0=0.053nm is the Bohr radius.

atom	a	$l_\perp$/m	$\frac{a}{l_\perp}$	ω_z/Hz	$\omega_\perp$/Hz	λ
^{87}Rb	$100a_0$	1.25×10^{-6}	4.33×10^{-3}	$2\pi\times211$	$2\pi\times74.6$	$\sqrt{8}$
^{7}Li	$-27a_0$	2.972×10^{-6}	4.8×10^{-4}	$2\pi\times117$	$2\pi\times163$	0.72
H	$4a_0$	1.606×10^{-6}	1.32×10^{-4}	$2\pi\times10.2$	$2\pi\times3.90$	2.61×10^{-3}

The density distribution of condensates without interatomic interaction is described in Figs.1 and 2. From the density distribution of ^{87}Rb confined in an anharmonic external potential shown in Fig.1(a), one sees that density distribution on the cross-section plane $r_{\perp 1}oz_1$ is close to an ellipse, of which the long axis is along the $r_{\perp 1}$ direction. From Fig.1(b), it is found that the central peak decreases as the anharmonic strength parameter ε increases although the shape of the profile is unchanged. It seems that the anharmonic strength is just like a weight on the top of the density peak. This result reveals that the density distribution of condensates is anisotropic which resembles those in harmonic potential of Ref.[15]. The density distributions of different condensates are depicted in Fig.2. There exists some difference for the central density of different condensates as shown in Fig.2(a). The highest peak is that of ^{87}Rb, the lowest one is that of H. This result is determined by the asymmetry parameter λ of condensates. Figure 2(b) shows that the density of ^{87}Rb along the radial direction expands larger than along z_1 axis; which results from $\lambda > 1$, whereas the density of ^{7}Li and H along the radial direction converges faster than along the z_1 axis because of $\lambda < 1$.

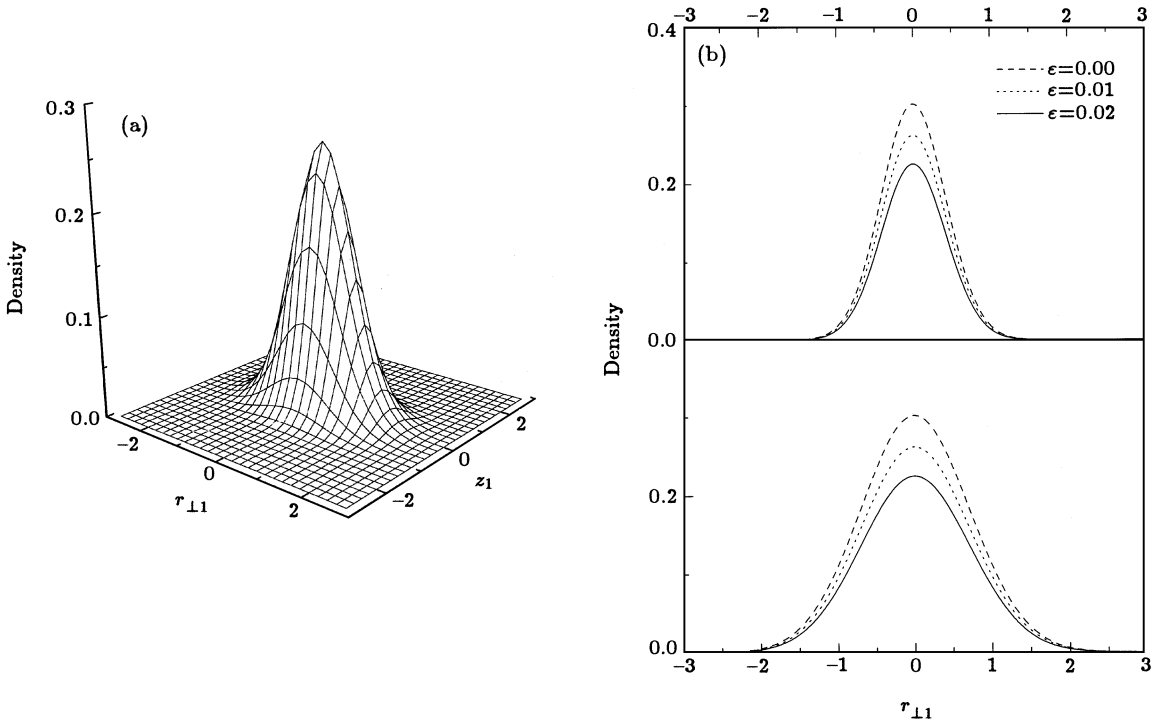


Fig.1. (a) The spatial distribution of the density for ^{87}Rb without interaction, with anharmonic parameter $\varepsilon = 0.01$. Distances are in units of $l_\perp$, major parameters are listed in Table 1. (b) Density distribution of ground state for ^{87}Rb along the radial direction (lower part) and z axis (upper part) in the noninteraction case.

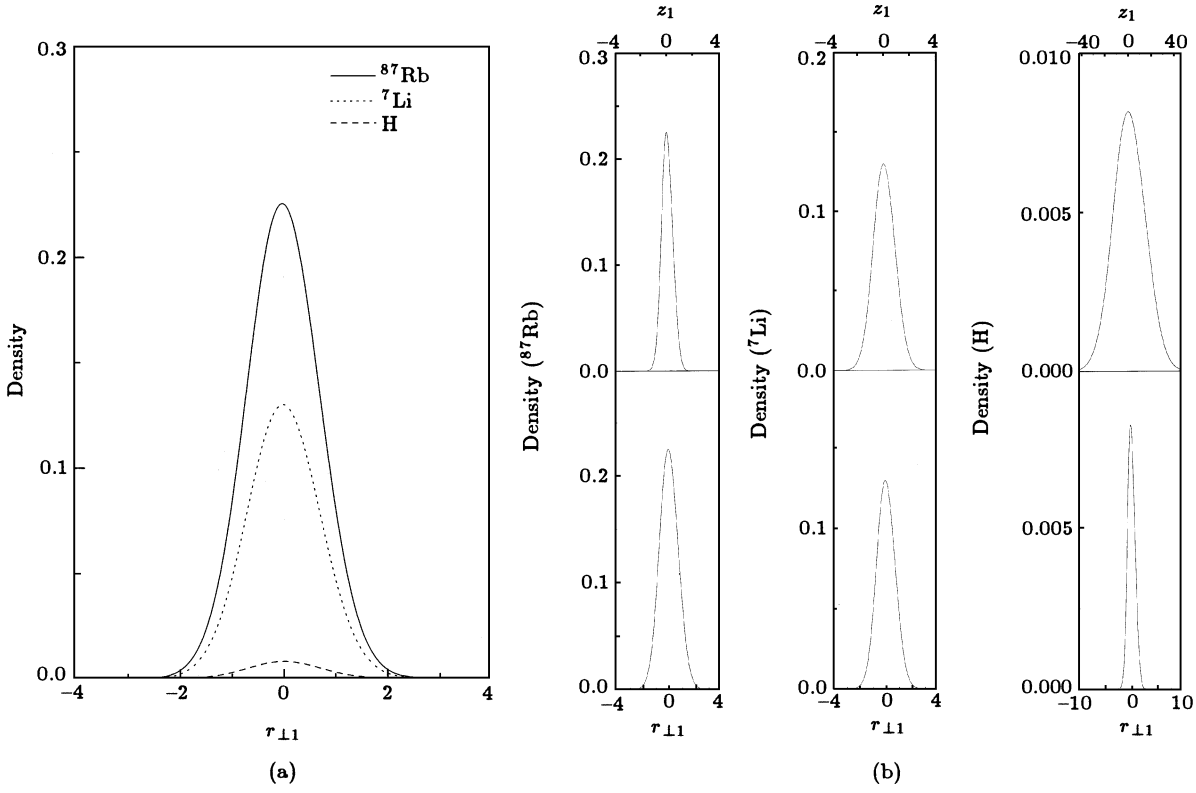


Fig.2. (a) Density of ground state wavefunction for the different atoms along the radial direction in the noninteraction case. (b) Density of ground state wavefunction for the different atoms along the radial direction (lower part) and the z axis (upper part) in the noninteraction case.

Figures 3 and 4 show the spatial distribution of condensates in the Thomas–Fermi model. In Fig.3(a), the curves with $\varepsilon = 0$ and $\varepsilon \neq 0$ represent the densities of external harmonic and anharmonic potentials, respectively. From the curve of $\varepsilon = 0$ in Fig.3(a), it is shown that the density distribution along $r_{\perp 1}(z_1)$ direction is an envelope peak. This kind of distribution is just as that of the condensate confined in a harmonic external potential in Ref.[15]. From Fig.3(a), we also see that as the anharmonic strength parameter ε increases to $\varepsilon = 0.02$, the central density decreases and the density distribution along $r_{\perp 1}(z_1)$ direction shows a double-well other than an envelope peak. This reveals that the anharmonic external potential has a pressing effect on the density distribution. Similarly, the spatial density distribution is given in Fig.3(b) which depicts

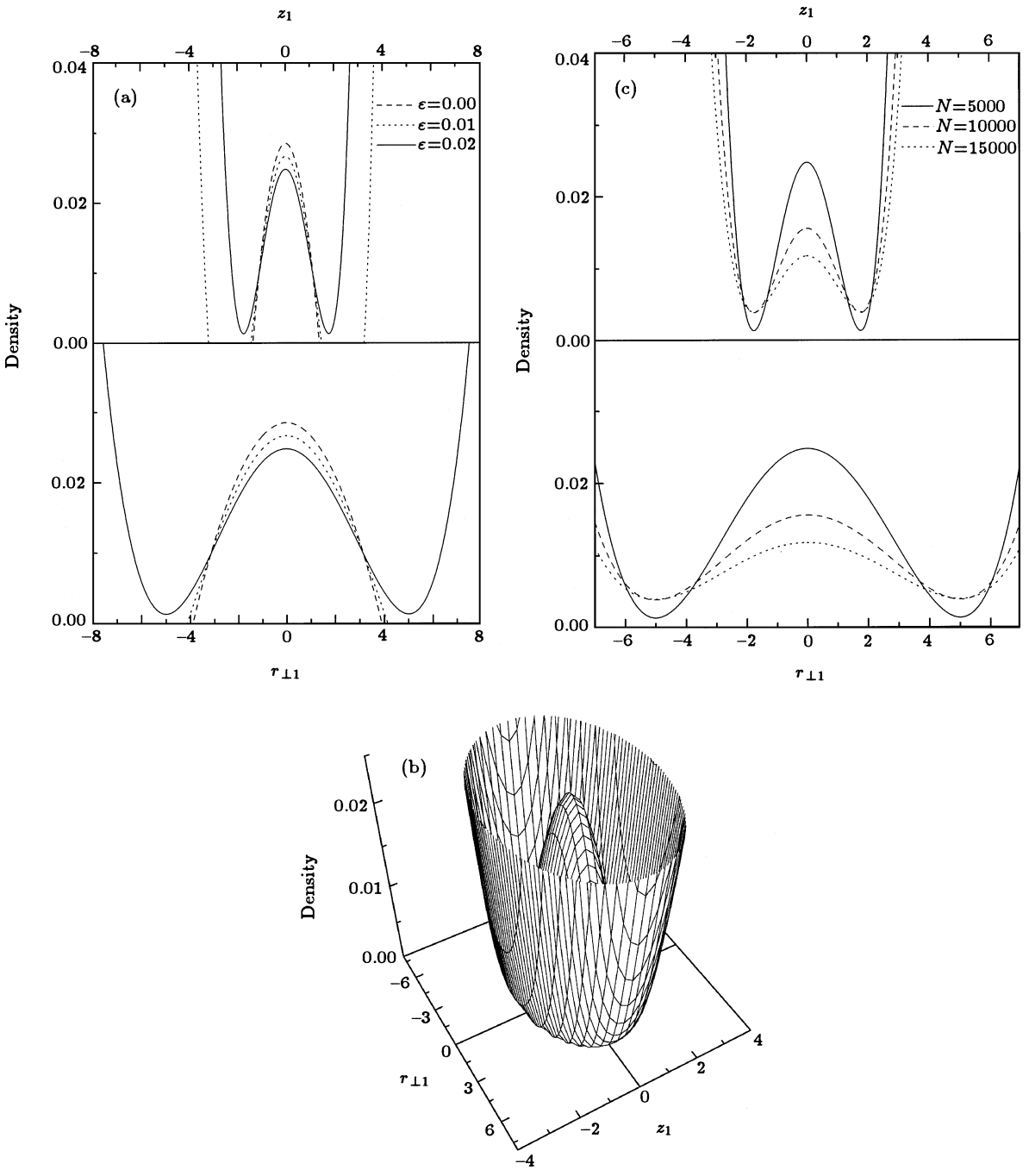


Fig.3. (a) Density distribution of ground state for ^{87}Rb along the radial direction (lower part) and z axis (upper part) in the strong interaction case ($N = 5000$). (b) The spatial distribution of the density for ^{87}Rb confined in a certain anharmonic strength ($\varepsilon = 0.02$) with strong interatomic interaction.(c) Density distribution of ground state for ^{87}Rb confined in a certain anharmonic strength ($\varepsilon = 0.02$) along the radial direction (lower part) and z axis (upper part) in the strong interaction case.

that the density distribution of the section cut by the $r_{\perp 1}oz_1$ plane is a double-asymmetric torus but not an ellipse as in the external harmonic trap case. Accompanying the increase of the number of atoms, the increase of interatomic interaction would press the density curve down into a flattened and lower one, as shown in Fig.3(c). For a fixed anharmonic strength, the distribution region of the condensate along the $r_{\perp 1}(z_1)$ direction enlarges as the number of atoms N increases, while the central density decreases [see Fig.3(c)]. Figure 4 shows the anisotropic distributions of condensates in Thomas–Fermi model. We find that the convergent ratio of condensate along the $r_{\perp 1}$ to that along the z_1 direction resembles that of interatomic noninteraction, although the density distributions are different from that of the noninteracting case.

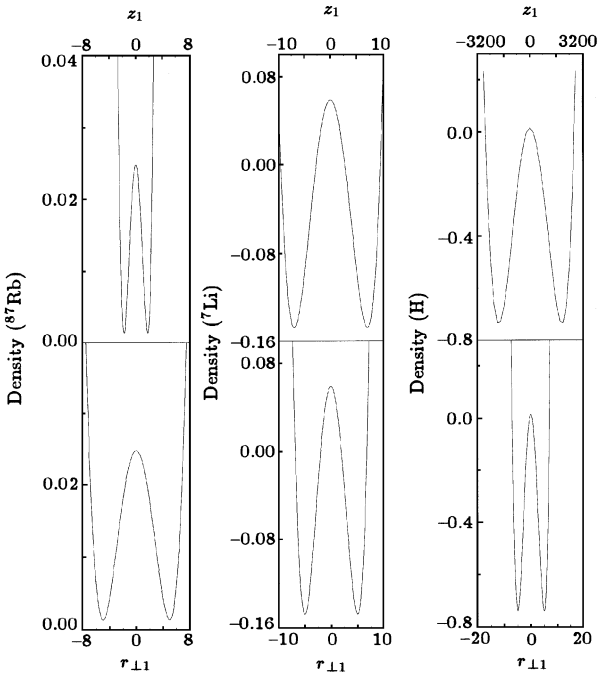


Fig.4. Density of ground state wavefunction for the different atoms along the radial direction (lower part) and z axis (upper part) in the strong interaction case.

It is worthwhile to point out that the chemical potential and the ground state energy of the condensates confined in an anharmonic external potential are lower than those in a harmonic potential, as can be seen from the expressions (14), (22) and (23). This means that BEC confined in an anharmonic external potential may be easily observed in the experiment. This might furnish us with an interesting topic of realizing experimental observation of BEC.

The aspect ratio of velocity distribution of condensate is shown in Figs.5 and 6. From Fig.5, one can see that the aspect ratios for both interatomic noninteraction and harmonic trap are unchanged as the number of atoms increases. By considering the strong interatomic interaction of condensates confined in an anharmonic external potential, the aspect ratio changes as the number of atoms increases. These results can also be obtained from the expressions (18) and (26). From Eqs.(16) and (17), without interatomic interaction, although the quantities $\langle x_1^2 \rangle$ and $\langle z_1^2 \rangle$ are functions of both asymmetry factor λ and anharmonic strength ε_1, the aspect ratio of velocity distribution R is only corrective with parameter $\sqrt{\lambda}$ [see Eq.(18)]. This indicates that, in weak interatomic interaction case, the effect of the anharmonic strength can be regarded as a small perturbation. For the strong interatomic interaction, however, the aspect ratio of velocity distribution R is a function of all the factors λ, ε_1 and μ_1 [see Eq.(26)]. Thus, the aspect ratio of the velocity distribution changes as the number of atoms increases. Figure 6 also shows the aspect ratios of different condensates for a fixed number of atoms ($N = 5000$). We can see that the aspect ratio of ^{87}Rb decreases as the anharmonic strength increases. However, the aspect ratios of ^{7}Li and H hardly vary with the change of anharmonic strength. For ^{87}Rb, when $\varepsilon = 0.08$, the aspect ratio $R \approx 2.78 < \lambda = 2.828$, which is closer to numerical result of Ref.[15].

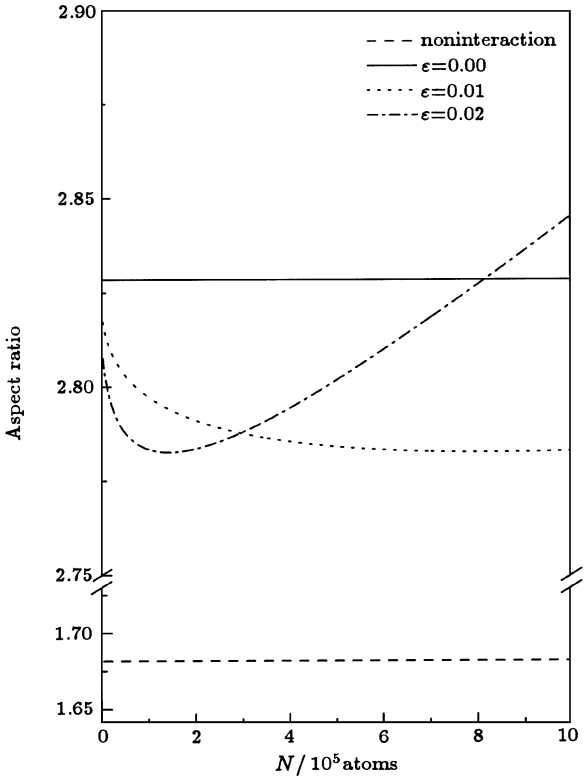


Fig.5. Aspect ratio of z axis to transverse (x–y) plane average velocity as a function of the number of atoms.

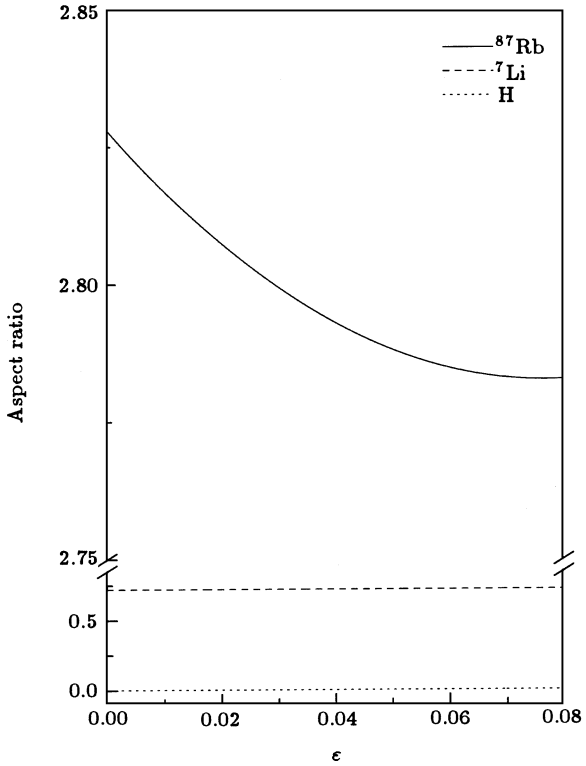


Fig.6. Aspect ratio for different atoms as a function of anharmonic strength.

6. Summary

In this paper, we have presented an anharmonic external potential to study the ground state properties of BECs. Two limiting cases on weak and strong interatomic interactions are discussed. For a weak interatomic interaction, we calculate the ground state wavefunctions and energy eigenvalues by means of variational approach combined with perturbation theory. It is shown that the aspect ratio of velocity distribution is only related to the asymmetric parameter $\sqrt{\lambda}$. As for strong interatomic interaction, we use the variational method combined with the Thomas-Fermi model to study ground state properties of BEC. It is shown that the aspect ratio is much closer to the numerical result. By comparing the ground state properties of different condensates, we find that the anharmonic strength has an important effect on the ground state properties of condensates. And both the ground state energy and the chemical potential of BEC confined in an anharmonic external potential are lower than those confined in harmonic one.

References

[1] Anderson M H, Ensher J R, Matthews M R, Wieman C E and Cornell E A 1995 *Science* **269** 198

[2] Davis K B, Mewes M O, Andrews M R, Druten N J, Durfee D S, Kurn D M and Ketterle W 1995 *Phys. Rev. Lett.* **75** 3969

[3] Bradley C C, Sackett C A and Hulet R G 1997 *Phys. Rev. Lett.* **78** 985

[4] Bradley C C, Sackett C A, Tollett J J and Hulet R G 1997 *Phys. Rev. Lett.* **79** 1170

[5] Bradley C C, Sackett C A, Tollett J J and Hulet R G 1995 *Phys. Rev. Lett.* **75** 1687

[6] Bradley C C, Sackett C A and Hulet R G 1997 *Phys. Rev.* A **55** 3951

[7] Cui H T, Wang L C and Yi X X 2004 *Acta Phys. Sin.* **53** 991 (in Chinese)

[8] Cai W Q, Li C W, Huo Y S and Wang Y Z 1999 *Acta Phys. Sin.* **48** 611 (in Chinese)

[9] Dalfove F, Giorgini S, Pitavskii L P and Stringari S 1999 *Rev. Mod. Phys.* **71** 463

[10] Pitaevskii L P and Eksp Z 1961 *Teor. Fiz.* **40** 646

[11] Pitaevskii L P and Eksp Z 1961 *Sov. Phys. JETP* **13** 451

[12] Pitaevskii L P and Eksp Z 1963 *J. Math. Phys.* **4** 195

[13] Parfins A S and Walls D F 1998 *Phys. Rep.* **303** 1

[14] Baym G and Pethick C J 1996 *Phys. Rev. Lett.* **76** 6

[15] Dalfovo F and Stringari S 1996 *Phys. Rev.* A **53** 2477

[16] Edwards M and Burnett K 1995 *Phys. Rev.* A **51** 1382

[17] Ruprecht P A, Holland M J, Burnett K and Edwards M 1995 *Phys. Rev.* A **51** 4704

[18] Yi X X 1999 *Acta Phys. Sin.* **48** 995 (in Chinese)

[19] Zhang S M and Ye F 1999 *Acta Phys. Sin.* **48** 977 (in Chinese)

[20] Wang D Z, Lu X H, Huang H and Li S Q 1999 *Acta Phys. Sin.* **48** 1192 (in Chinese)

[21] Yan K Z and Tan W H 1999 *Acta Phys. Sin.* **48** 1185 (in Chinese)

[22] Tan W H and Yan K Z 1999 *Acta Phys. Sin.* **48** 1983 (in Chinese)

[23] Yan K Z and Tan W H 2000 *Acta Phys. Sin.* **49** 1909 (in Chinese)

[24] Andrews M R, Kurn D M, Miesner H J, Durfee D S, Townsend C G, Inouye S and Ketterle W 1997 *Phys. Rev. Lett.* **79** 553

[25] Anderson B P and Kasevich M A 1998 *Science* **282** 1686

[26] Spekkens R W and Sipe J E 1999 *Phys. Rev.* A **59** 3868

[27] Pu H, Zhang W P and Meystre P 2002 *Phys. Rev. Lett.* **89** 090401

[28] Kittel C and Kroemer H 1980 *Thermal Physics* (W. H. Freeman and Co., New York)

[29] Spekkens R W and Sipe J E 1998 *Prog. Phys.* **46** 873

[30] Search C P, Rojo A G and Berman P R 2001 *Phys. Rev.* A **64** 013615

[31] Goldstein E V and Meystre P 1997 *Phys. Rev.* A **55** 2935

[32] Wadati M and Tsurumi T 1999 *J. Phys. Soc. Japan.* **68** 3840

[33] Tsurumi T and Wadati M 2001 *J. Phys. Soc. Japan.* **70** 1512

[34] Fried D G, Killian T C, Willmann L, Landhuis D, Moss S C, Kleppner D and Greytak T J 1998 *Phys. Rev. Lett.* **81** 3811